Chalcogenide Letters

Tech Science Press

http://doi.org/10.32604/cl.2026.082607

ARTICLE

Influence of Germanium Substitution on the DC Electrical Properties and Energy Density of States in $Pb_{50-x}Ge_xTe_{50}$ Ternary Chalcogenide Alloys

Muayed Khaleel Ibrahim[1], Shaymaa Hashim Aneed[2], Nidhal Saleh Mohammed[2], Kareem Ali Jasim[2] and Mudatheer M. Al-Slivani[3,*]

[1]Department of Energy Engineering, College of Engineering, University of Baghdad, Baghdad, Iraq
[2]Department of Physics, College of Education for Pure Sciences, Ibn Al-Haitham, University of Baghdad, Baghdad, Iraq
[3]Department of Physics, College of Education for Pure Sciences, Al-Furqan University, Mosul, Iraq
*Corresponding Author: Mudatheer M. Al-Slivani. Email: mudatheeralslivani@gmail.com

Received: 19 March 2026; Accepted: 04 June 2026; Published: 07 August 2026

ABSTRACT: This study investigates the structural evolution and DC electrical properties of $Pb_{50-x}Ge_xTe_{50}$ ternary chalcogenide alloys with varying germanium concentrations (x = 5, 10, 15, 20). Synthesized via the melt-quenching technique, the alloys were characterized using Scanning Electron Microscopy (SEM) and temperature-dependent electrical resistivity measurements within the range of 290–475 K. Microstructural analysis revealed that increasing Ge substitution significantly promotes matrix densification, reducing porosity and improving inter-granular connectivity. The DC conductivity exhibits a systematic increase with Ge content up to x = 15, attributed to the increased density of defect states. For instance, as Ge content increases from x = 5 to x = 15, the DC conductivity increases, corresponding to an activation energy (ΔE_1) shift from 0.203 eV to 0.281 eV at high temperatures. However, for the sample with x = 20, a non-monotonic shift in conductivity parameters is observed, evidenced by a significant reduction in the pre-exponential factor (σ_{01}) compared to the intermediate compositions, which indicates a alteration in the conduction pathways. The conduction data were analyzed using the Mott and Davis model, identifying three distinct mechanisms: hopping between localized states near the Fermi level at low temperatures, hopping within band-tail states at intermediate temperatures, and excitation into extended states at high temperatures. Furthermore, calculations of the density of states (DOS) indicated that Ge incorporation increases the density of extended and localized states while simultaneously narrowing the band tail width (ΔE), thereby reducing structural randomness. These findings highlight the efficacy of germanium doping in tuning the electronic structure of Pb-Ge-Te alloys, suggesting their suitability for advanced optoelectronic and semiconductor applications.

KEYWORDS: Chalcogenide alloys; $Pb_{50-x}Ge_xTe_{50}$; DC conductivity; Mott and Davis model; density of states; germanium doping

1 Introduction

Chalcogenide materials containing one or more elements from Groups IV to VI (elements such as tellurium (Te), selenium (Se), sulfur (S), or polonium (Po)) have recently received considerable attention due to their unusual properties, including anharmonic effects, poor lattice thermal conductivity, unparalleled thermoelectric performance [1,2], complex band structures, high chemical power coefficient, chemical stability, and low toxicity [3,4]. Some of these compounds exhibit paraelectricity, ferroelectricity, and superconductivity [5–7].

Chalcogenide materials have garnered significant interest across various industrial sectors due to their versatile properties. However, once materials with the desired properties are obtained and tailored to specific uses, significant progress is expected. Although these materials will enable many new applications, not all of their properties can be derived directly from binary materials or manufactured raw components. Therefore, combining two or more elements to form an alloy is the most common and simplest way to modify their properties [8].

The alloys of tellurium based on Germanium have a large stoichiometric deviation of the tellurium element. The primary non-chemical defects are divalent ionic vacancies of metals. Due to such a stoichiometric deviation, GeTe always portrays sp-type conductivity. Doping of GeTe with electrochemical impurities of donor type is required to decrease the concentration of holes and attain the best thermoelectric characteristics. When GeTe is dissolved in Bi_2Te_3, it serves as a donor. Better performance in thermoelectric should be achieved with $(Pb, Sn)_{1-x}Ge_2Te$ alloys [9,10].

Such alloys may be engineered to have better electronic properties, and have lower lattice thermal conductivity than SnTe, PbTe and GeTe. Moreover, these alloys are able to reduce the phase transition temperature to lower than operating temperature of the thermoelectric device to enhance stability [11]. Partial replacement of lead with germanium was selected to: (i) tune the energy band gap (ii) capability to control energy band gap, (iii) implementation of directed average lattice defects in the system and (iv) improvement in conduction process.

Studying the composition dependence of these alloys is crucial, as it allows researchers to precisely map the solubility limits and identify the exact stoichiometric ratios that yield optimal carrier mobility and minimal thermal conductivity for device integration. It makes $Pb_{50-x}Ge_xTe_{50}$ alloys even more valuable in high-end applications, as the adjustment of both electrical and structural properties can be precisely done. The study of the effects of germanium on electrical conductance and energy density inter $Pb_{50-x}Ge_xTe_{50}$ alloys may be artificially chosen perhaps because germanium doping can greatly change the conduction behavior and electronic structure in materials. One can vary, by adding germanium to the alloy matrix, properties such as density of states and transport of charge carriers that can be studied [12], which are important in order to investigate the characteristics of a semiconductor material. The specific electronic properties of the Ge can produce an effect on energy band gap and interferes with distribution of both well-localized and extended energy state (one of the most important factors that control the electrical conducting capabilities) [13].

Hence this study is intended to investigate systematically the effect of lead (Pb) replacement by germanium (Ge) on the DC electrical properties and the energy densities of states in ternary $Pb_{50-x}Ge_xTe_{50}$ alloys. By preparing the compositions with different germanium concentrations (x = 5, 10, 15, and 20 at. %) and studying their temperature-dependent conductivities (for the range 290–475 K) in order to provide information on the conduction mechanism. The significance of this work is to understand how doping by Ge can be used in order to tailor the energy band gap, induce controlled defects and heavily modify its electronic structure. Finally, this work investigates the scope for control over both electrical and structural properties of such chalcogenide alloys for high application-centred, advanced semiconductor and optoelectronic devices.

2 Experimental Details

The ternary mixture of $Pb_{50-x}Ge_xTe_{50}$ was produced through melting point technique. $Pb_{50-x}Ge_xTe_{50}$ alloys containing germanium concentrations of 5, 10, 15 and 20 were produced using high-purity lead, tellurium and germanium powders, 99.999 percent pure. The raw materials were weighed according to

their atomic mass percentages of the elements and the concentration of the elements used in the alloy in order to achieve uniform proportions. The process of mechanical grinding was conducted using a planetary ball mill (Model PM 100, RETSCH, Germany) for 50 min was conducted using a mechanical vibrator" or "ball mill in 50 min. Each sample was finely crushed and pressed into pellets under a pressure of 5 t/cm^2 using a standard hydraulic press (Specac Atlas 15T, UK). The samples were put in separate capsules that were vacuumed at 10^{-3} bar and then sealed. The method was employed to maintain quality of the end alloy, avoid contamination and have a perfect control over the levels of activation. The capsules were put in an electric furnace and the samples heated to 1100°C in five hours. Following heat treatment, Following heat treatment, the sealed vacuumed quartz capsules were rapidly quenched in air. The material remained strictly sealed inside the vacuumed environment (10^{-3} bar) during the entire cooling process to completely prevent ambient exposure, oxidation, and the formation of oxygen vacancies. The ingots were pressed into fine and pressed them with a hydraulic press in 6 t per square centimeter. The samples were shaped into 1.5 cm diameter discs and 3 mm in thickness. The crushed samples were put back in the furnace at 200°C with 2 h of time until they cooled to room temperature. The samples were cooled and then ready to analysis. This meticulousness allowed even distribution of germanium in the $Pb_{50-x}Ge_xTe_{50}$ matrix allowing to characterize the impact of germanium on the conduction mechanisms and the structural properties. Measurements of electrical resistivity that are dependent on temperature [14,15].

Surface morphology analysis was performed to study the structural properties of the sample surfaces. The electrical resistivity is measured by clamping the sample between two copper electrodes using a special designed holder and then the sample should be put in an electric furnace as seen in Fig. 1. A Keithley-type electrometer (Model 2400 Source Meter, Keithley Instruments, USA) is connected to measure the voltage and current passing via the sample and give proper readings. To have an accurate temperature reading, the furnace temperature is steadily raised in 10 K steps until it attains a temperature of 475 K. Current and voltage are recorded at every temperature step and electrical resistivity and conductivity of the sample is determined versus temperature. This arrangement guarantees that the data of conductivity analysis is accurate. The estimated instrumental error for electrical resistivity measurements was within ±3%, and temperature control accuracy was ±1 K.

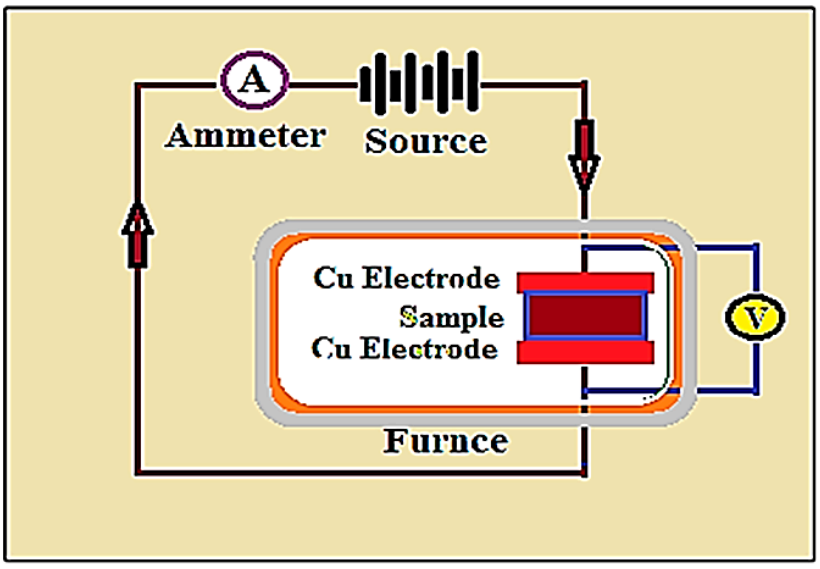

Figure 1: A schematic diagram of the electrical resistivity measurement apparatus.

3 Results and Discussion

The surface morphology of the prepared $Pb_{50-x}Ge_xTe_{50}$ alloys was probed to determine the structural evolution caused by the substitution of germanium probed by scanning electron microscopy (SEM; JEOL JSM-IT500, Japan). Fig. 2 shows the changes in microstructures as a function of the compositional spectrum. The micrographs reveal a amorphous structure characterized by granular agglomeration and glassy matrix formations. As seen in Fig. 2a for the low-concentration specimen (x = 5), the surface is relatively porous, made up of smaller and fairly irregularly shaped grains, which are indicative of a stochastic chalcogenide matrix. As the germanium fraction increases to x = 10 (Fig. 2b) and x = 15 (Fig. 2c), there is a strong change in the appearance of the surface topology: the density of voids decreases significantly, and a qualitative tendency toward the refinement of grains and an increase in inter-granular connection is observed. For the highest concentration at x = 20 (Fig. 2d), this matrix densification is highly pronounced. This densification is critical, as it likely facilitates charge transport processes by reducing the scattering centres related to the structural disorder. These enhancements in the grain packing and attenuated porosity on the SEM images are consistent with the later electrical performance measurements that support the speculation that Ge-doping is an effective suppressor of structural randomness and improves conduction pathways.

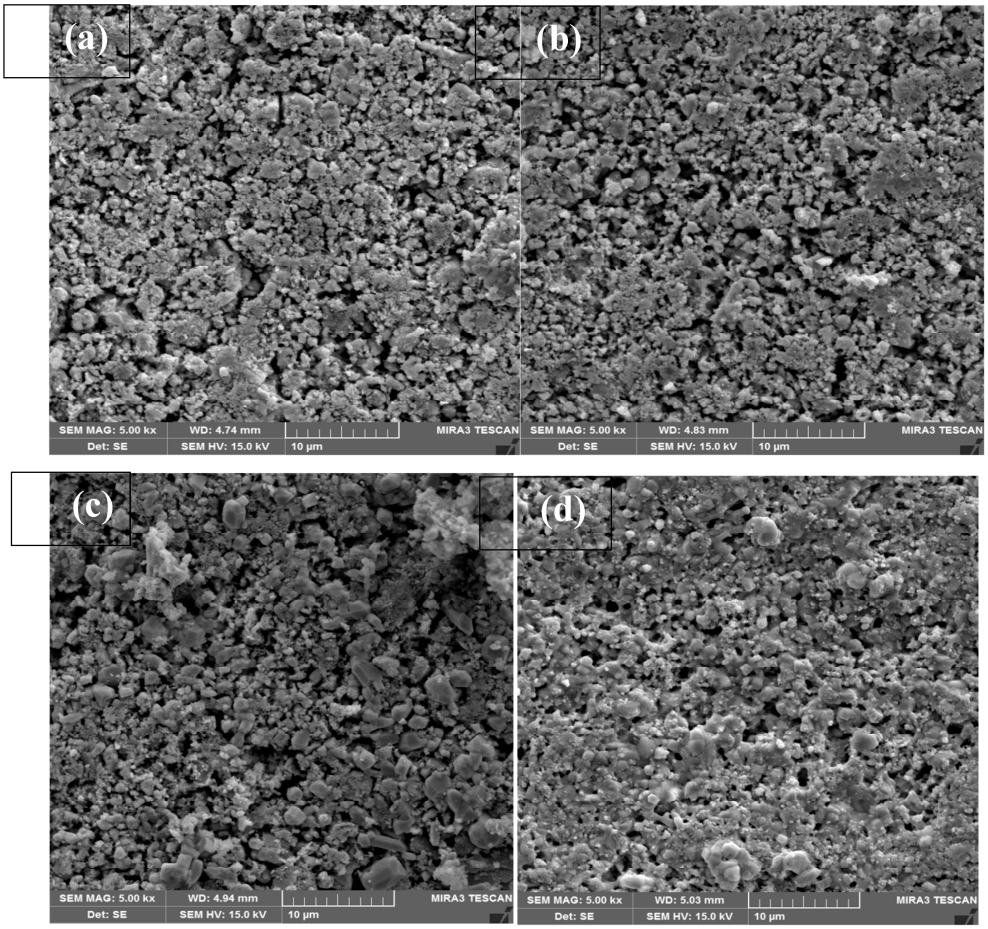

Figure 2: Scanning Electron Microscopy (SEM) micrographs exhibiting the surface morphology and microstructural evolution of $Pb_{50-x}Ge_xTe_{50}$ ternary alloys with different Germanium concentrations at: (**a**) x = 5, (**b**) x = 10, (**c**) x = 15, and (**d**) x = 20.

The DC resistance and conductivity of four samples of a $Pb_{50-x}Ge_xTe_{50}$ ternary alloy at the concentrations of germanium x = 5, 10, 15, and 20, as a function of temperature, were investigated in the temperature range 290–475 K. The experiment data was well captured in this temperature range using the thermally activated process model.

All alloys exhibit semiconductor behavior, i.e., their conductivity increases with increasing temperature, as shown in the thermal conductivity curves. This indicates that the higher the germanium concentration in the alloy, the higher the electrical conductivity. This indicates that the electrical conductivity of the $Pb_{50-x}Ge_xTe_{50}$ system increases as the germanium concentration increases. It is also noted that there is a difference or variation in the behavior of the curves with different temperature ranges, depending on the conductivity patterns at different temperature ranges. Conduction may be due to electrons bouncing between energy levels near the Fermi level, which occurs at low temperatures, or jumping between distant levels at medium and high temperatures. These results are consistent with the Mott and Davis model, which assumed that continuous electrical conduction in random semiconductors (random chalcogenides) has three conduction mechanisms (at different temperatures: low, medium, and high) according to the following relationship [16,17].

$$\sigma = \sigma_{01} e^{\left(-\frac{\Delta E_1}{k_\beta T}\right)} + \sigma_{02} e^{\left(-\frac{\Delta E_2}{k_\beta T}\right)} + \sigma_{03} e^{\left(-\frac{\Delta E_3}{k_\beta T}\right)} \quad (1)$$

where σ_{01}, σ_{02}, and σ_{03} are the pre-exponential factors, ΔE_1, ΔE_2, and ΔE_3 are the activation energies for DC conduction, T is absolute temperature and k_β is Boltzmann's constant.

With increasing germanium concentrations, the electrical conductivity of $Pb_{50-x}Ge_xTe_{50}$ alloys increased significantly (x = 5, 10, 15, 20). All alloys exhibited semiconducting behavior, with conductivity growing considerably with temperature, according to the data. Three distinct conduction regions were identified by the relationship between conductivity and temperature: low, intermediate, and high temperatures [18]. Electrical conduction between localized states near the Fermi level determines conductivity in the low-temperature range. Electrical conduction in the intermediate-temperature region dominated conduction at low temperatures, which was influenced by the high density of band-tail states resulting from germanium doping. The transfer of charge carriers between extended states increased electrical conductivity at high temperatures, while germanium increased the activation energy required for these changes. The germanium doping also decreased the width of the energy tail (ΔE), which improved the hopping distances (R) and the Atomic distance (a) [19]. As shown in Tables 1 and 2.

By calculating the logarithm of both sides of Eq. (1), the relationship between ln logarithm σ_{dc} and 1000/T can be plotted, identifying three distinct regions with different slopes. These regions show the dominance of distinct conduction mechanisms in specific temperature ranges. These slopes correspond to the three terms in Eq. (1), which represent different conduction modes [20]. Three distinct regions can be seen in the plot of the relationship between logarithm σ_{dc} and 1000/T when examining ternary alloy samples of $Pb_{50-x}Ge_xTe_{50}$ graphically with Germanium concentrations x = 0, 5, 10, 15, and 20, as shown in Fig. 3.

The curves generated by three linear parts by each of the four samples were plotted in the graph of Fig. 3 (representing the relationship between the logarithm of the conductivity and 100). At low temperature (290–340 K), the original conduction zone does not need much energy to allow the electrons to hop between Fermi levels. Second conduction is electron hopping between the tail of the density of states by mechanisms involving localized states in the intermediate temperature range between 340 and 390 K and finally conductors are accessed by transition to the third conduction region at high temperatures between 390 and 475 K where transitions between extended states of the conduction band and the valence band

occurs. It is possible to observe three distinct linear regions of the lnsigma dc variation vs. 1000/T per alloy sample. The steepnesses of these lines are computed to obtain the two activation energies ΔE_1, ΔE_2 and ΔE_3 at every temperature interval. Also, using the extrapolation of each line to the intercept with the y-axis, the pre-exponential terms σ_{01}, σ_{02}, and σ_{03} can be obtained. The factors before the exponential are determined by values at which each of the lines crosses the y-axis, which are lnN00N with N being 1, 2 or 3. Energies of activation and pre-exponential factors of each of the samples in each of the three temperature ranges were determined and have been tabulated in Table 1.

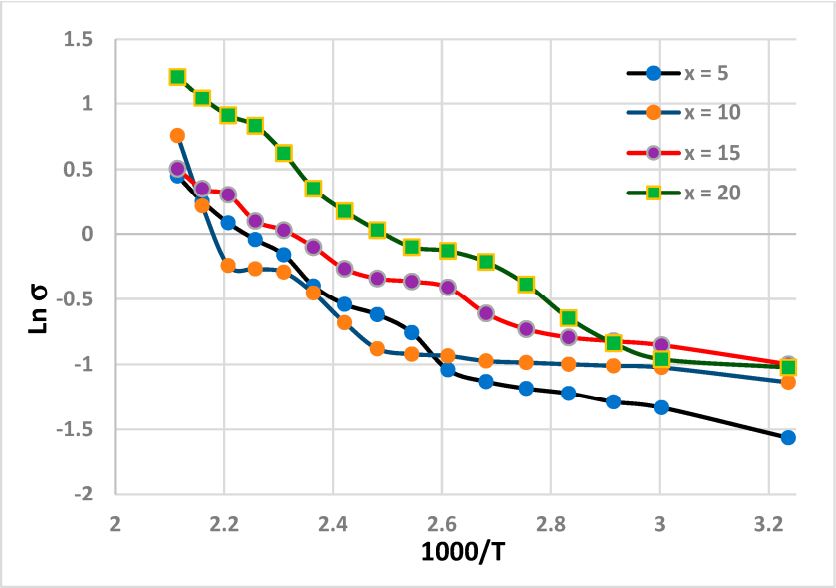

Figure 3: lnσ_{dc} as a function of (1000/T) for $Pb_{50-x}GexTe_{50}$ ternary alloy samples with Germanium concentrations x = 5, 10, 15, and 20.

The high-temperature semiconductor region is considered to be the first one, which is located between 390 K and 475 K. This value is the initial term of Eq. (1). At this high temperature regime, the carrier density is equal to the intrinsic carrier density. The conductivity in this region is based on two key factors; sample temperature and lattice vibrations. The more the temperature is raised, the greater the number of free carriers in the material and the higher the conductivity of the material. The lattice vibrations however bring about phonon which interacts with the electrons, which results in the electron-phonon interactions. These interactions can decelerate the movement of electrons and take more energy to be activated. Consequently, the activation energy in the first region is significantly higher [21]. The latter section of the curves describes the intermediate range of temperature between 340 and 390 K. This area is semiconducting in nature. In this range, the carrier and intrinsic carrier density are equal. The DC resistance in this region varies with the concentration, mean free path, and carrier mobility. This variation is due to the small crystal size and poor crystallinity. Conductivity decreases due to surface defects, dislocations, and structural distortions, which cause randomization in the crystal structure, leading to the emergence of levels within the energy gap at the tails of the conduction and valence bands, according to previous studies. The low-temperature range, extending from 290 to 340 K, is described as the third limit of the curves. The ionization of impurity atoms affects the conductivity of this region. Due to the thermally assisted movement of carriers between localized states at the Fermi level, conduction occurs at low temperatures between localized levels close to the Fermi level [21]. There is a distinct drop in the pre-exponential factor (σ_{02}) for the x = 20 sample

compared to the x = 10 and x = 15 compositions. This variation highlights that the optimal enhancement of transport parameters is bounded between x = 10 and x = 15, beyond which excessive Ge addition alters carrier mobility.

Table 1: Activation energies and pre-exponential factors (σ_0) dependent on composition of three conduction areas in $Pb_{50-x}Ge_xTe_{50}$ alloys (x = 5, 10, 15, 20).

x	ΔE_1 (eV)	σ_{01} $(\Omega\cdot cm)^{-1}$	ΔE_2 (eV)	σ_{02} $(\Omega\cdot cm)^{-1}$	ΔE_3 (eV)	σ_{03} $(\Omega\cdot cm)^{-1}$
5	0.203	7.2e−5	0.104	1.2e−9	0.012	6.9e−10
10	0.276	5.4e−3	0.181	1.7e−5	0.031	2.8e−7
15	0.281	5.1e−3	0.189	2.3e−9	0.020	3.3e−10
20	0.252	1.4e−6	0.170	1.8e−7	0.15	7.7e−8

The density of extended states in the conduction and valence bands and the density of localized states in the tails of the energy bands and near the Fermi level within the energy gap were calculated using Eqs. (2)–(4) below given in, after substituting the pre-exponential factor (σ_{01}, σ_{02}, and σ_{03}), for each sample parameters in Table 1, the electron charge (e), the phonon frequency (ν_{ph}) set at 10^{13} s^{-1} [22], and the hopping distance (R) which is given by Eq. (5) [16,17]. Table 2 shows the calculations for all $Pb_{50-x}Ge_xTe_{50}$ ternary alloy samples with Germanium concentrations x = 0, 5, 10, 15, and 20.

$$N(E_{ext}) = \left[\frac{6m}{e^2\hbar}\right]\sigma_o(ext) \tag{2}$$

$$N(los) = \left[\frac{6}{e^2 V phR^2}\right]\sigma_o(los) \tag{3}$$

$$N(E_F) = \left[\frac{6}{e^2 V phR^2}\right]\sigma o3 \tag{4}$$

$$R = 0.7736\left[\frac{\Delta\alpha^{-1}}{N(E_{ext})(kT)^2}\right]^{0.25} \tag{5}$$

In chalcogenide glasses, especially those in which the group VI elements are present in large fraction, the valence band is made up of the lone pair electrons [22]. The first work on the effect of additives on the properties of V-VI alloys was by Kastner, who observed that the additives modify the tail width in the valence band. In particular, valence electrons that are located close to the more electropositive atoms have greater energies than the valence electrons located close to the more electronegative atoms [23]. Also, the alteration of the tail of the conduction band is due to the variation in the bond type in the alloy [24]. It is not always symmetrical that the band is broadened and it could lead to changes in the conduction band edge [18]. It, in its turn, affects the densities of localized states $N(E_{loc})$, extended states $N(E_{ext})$, and states close to the Fermi level $N(E_F)$ [15]. These are manifested in the findings reported in Table 2 and Fig. 4 indicating the effects of the alloy composition on the electronic properties by changing state densities and band structure.

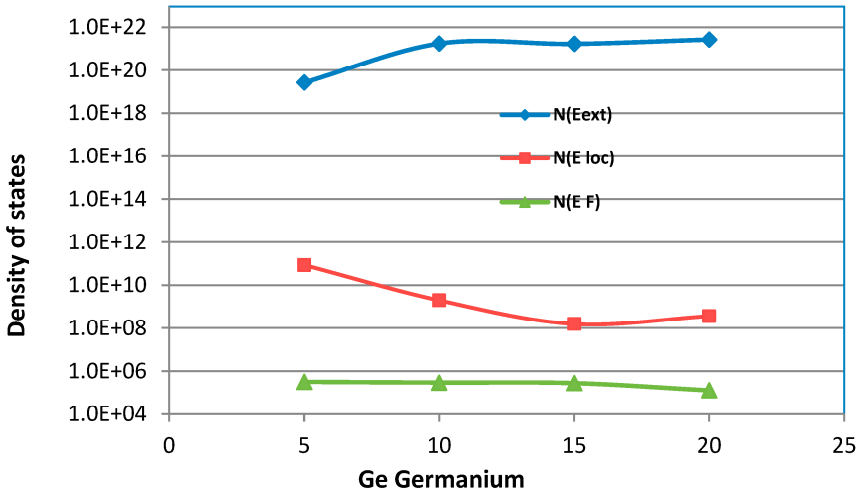

Figure 4: Densities of states as a function of Germanium concentrations for $Pb_{50-x}Ge_xTe_{50}$ alloy samples with x = 5, 10, 15, and 20.

It is noted from Table 2 that all values of the extended and localized densities of states in the tails and near the Fermi level were significantly affected by the partial substitution of tellurium by germanium, as both the conduction and valence bands were affected by changes in the atomic sizes of the substituent elements [24]. This is because in chalcogenide glasses, the valence band consists of lone pair electrons [22,25]. The influence of additives on the properties of V-VI alloys was first discussed by Kastner, who observed that width of the valence band tail is influenced by the additives. Particularly the valence electrons that are located near electronegative atoms are found to be higher in energy than those near less electronegative atoms. In addition, changes in the conduction band tail result from differences in the types of bonds within the alloy [25,26]. The band width is not necessarily uniform and this can result in the shifts on the conduction band edge [25–27]. This further influences the densities of localized states $N(E_{loc})$, extended states $N(E_{ext})$ and states near Fermi density $N(E_F)$ [28]. The latter are manifested in the findings which are provided in Table 2 and indicate how the alloy mixture influences the electronic properties by affecting the band structure and state densities.

Table 2: The relationship between the composition and various parameters such as the density of extended states $N(E_{ext})$, localized states $N(E_{loc})$, density at the Fermi level $N(E_F)$, tail width ΔE, hopping distance R, and the parameter aaa has been studied as a function of the Germanium concentration in $Pb_{50-x}Ge_xTe_{50}$ ternary alloy samples, with values of 5, 10, 15, and 20.

x	(eV)	R (A^0)	a (A^0)	$N(E_{ext})$ ($eV^{-1}\cdot cm^{-3}$)	$N(E_{loc})$ ($eV^{-1}\cdot cm^{-3}$)	$N(E_F)$ ($eV^{-1}\cdot cm^{-3}$)
0	0.105	0.03	6.061	5.92e16	8.94e10	8.27e7
5	0.099	0.012	0.02	2.655e19	8.46e10	3.25e5
10	0.095	0.028	0.0019	1.74e21	1.98e9	2.97e5
15	0.092	0.035	0.002	1.69e21	1.56e8	2.81e5
20	0.082	0.017	0.068	2.7e21	3.67e8	1.29e5

Replacement of part of terylium by germanium has a strong impact on the energy density by altering the band structure, decreasing the band gap, and creating regulated defects. This adjustment customizes the densities of energy in the extended, localized and Fermi states. Parameters like tail width (ΔE) and hopping distance (R), interlayer spacing and other parameters associated with conductivity show significant

variation with enhanced electronic properties and energy storage capabilities. In general, germanium doping increases electrical conductivity and energy densities of alloys studied and thus, they are promising candidates in the development of future semiconductor and optoelectronic devices [28,29]. The tails become narrower with an increase in concentration of germanium in $Pb_{50-x}Ge_xTe_{50}$ alloys leading to a decrease in the randomness of the crystal structure as illustrated in Fig. 5 indicating the dependence of the width of the tails of the energy bands on the concentration of germanium.

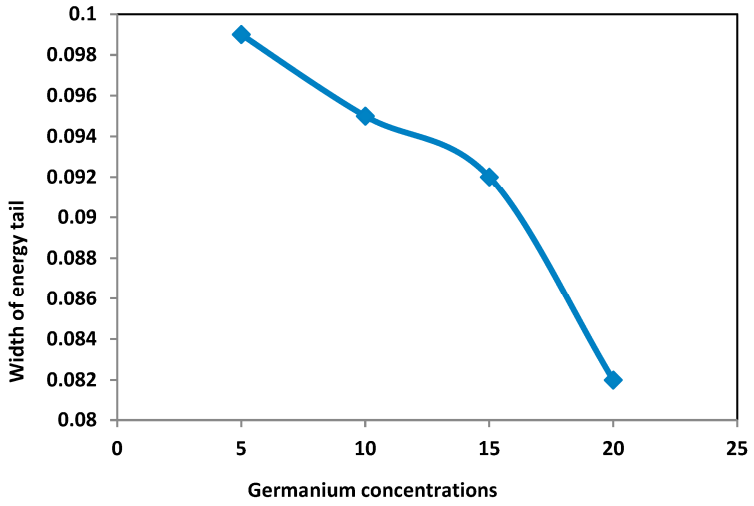

Figure 5: Width of the tails (ΔE) as a function of Germanium concentrations for $Pb_{50-x}Ge_xTe_{50}$ alloy samples with x = 5, 10, 15, and 20.

Germanium doping significantly influences the electrical conductivity and energy density states of alloys by altering the electronic structure and conduction pathways. Germanium substitution decreases the energy gap, increases the density of extended states, and localizes them closer to the Fermi level, thereby improving the mobility of charge carriers. The exponential rise in electrical conductivity with temperature can be attributed to the rearrangement of alloy atoms and the reduction of structural randomness, aligning with the hopping mechanism in both localized and extended states within the conduction band.

The systematic enhancement in DC electrical conductivity observed for compositions up to x = 15 is attributed to the structural modification of the PbTe lattice, where the substitution of Pb atoms with smaller Ge atoms likely increases the local disorder and the density of localized states near the Fermi level ($N(E_F)$). This modification facilitates carrier hopping and supports the premise that controlled doping optimizes electronic transport by tuning the band structure, as observed in recent investigations into chalcogenide alloys [30]. However, the distinct reduction in conductivity and the pre-exponential factor at x = 20 suggests that the Ge concentration has exceeded the solubility limit within the matrix. As explicitly demonstrated in Table 1, there is a sharp drop in the pre-exponential factor (σ_{01}) for the x = 20 sample, which falls drastically from 5.1×10^{-3} $(\Omega\cdot cm)^{-1}$ at x = 15 down to 1.4×10^{-6} $(\Omega\cdot cm)^{-1}$ at x = 20. This severe decline provides clear evidence of a disruption in the conduction pathways. At this high concentration, it is hypothesized that the system approaches its solubility limit, potentially leading to local structural inhomogeneities or Ge-rich clustering as suggested in similar systems, which could act as scattering centers for charge carriers, creating structural inhomogeneities that act as scattering centers for charge carriers. This behavior does not support the continuity of the enhanced hopping mechanism observed at lower concentrations but instead aligns

with the mechanism where excessive defect density and secondary phase precipitates drastically reduce carrier mobility and degrade overall transport properties [30].

The current results about the enhancement of the DC conductivity and the simultaneous structural upgrading with the rise of the Germanium content is in agreement with the latest trends that have been reported in similar chalcogenide systems. Germanium replacement increases the density of extended states, but suppresses structural disorder, which is consistent with our findings of reduced porosity and increased inter-granular connectivity in PbGeTe alloys [26]. The improvement in electrical performance caused by defect engineering through the Germanium doping is also in line with the findings of Zhao et al. (2025), who established that the addition of Germanium to the chalcogenide matrix is an effective way of tuning the electronic structure and enhancing charge-transport efficiency [31].

It is important to emphasize that the demarcation into low, intermediate, and high-temperature zones refers strictly to distinct electronic transport regimes governed by different activation mechanisms within the framework of the Mott and Davis model, rather than thermodynamic phase transitions.

4 Conclusion

This investigation into the DC electrical properties of $Pb_{50-x}Ge_xTe_{50}$ ternary chalcogenide alloys successfully demonstrates that substituting lead with germanium significantly enhances the material's electrical performance. The study confirmed that all alloy compositions exhibit characteristic semiconducting behavior, with electrical conductivity increasing as a function of temperature over the 290–475 K range. A key finding is the direct relationship between germanium concentration and electrical conductivity; as more germanium was added, the conductivity of the alloys systematically increased. Analysis of the temperature-dependent conductivity, guided by the Mott and Davis model, revealed three distinct conduction mechanisms operating in different temperature regions: carrier hopping between localized states near the Fermi level at low temperatures, hopping between band-tail states at intermediate temperatures, and transitions in extended states at high temperatures. Specifically, at high temperatures, the activation energy varied from 0.203 eV (x = 5) to 0.281 eV (x = 15), while the density of extended states increased from 2.655×10^{19} to 1.69×10^{21} eV^{-1} cm^{-3}. The addition of germanium was found to fundamentally alter the electronic structure by increasing the density of states while simultaneously narrowing the band tail width, indicating a reduction in the material's structural randomness. These findings underscore the efficacy of germanium doping as a method to precisely tune the electronic properties of these alloys, establishing them as highly promising candidates for the development of advanced semiconductor and optoelectronic devices.

Acknowledgement: Not applicable.

Funding Statement: The authors received no specific funding for this study.

Author Contributions: The authors confirm contribution to the paper as follows: Conceptualization, Muayed Khaleel Ibrahim and Mudatheer M. Al-Slivani; methodology, Shaymaa Hashim Aneed; validation, Nidhal Saleh Mohammed and Kareem Ali Jasim; formal analysis, Muayed Khaleel Ibrahim and Shaymaa Hashim Aneed; investigation, Nidhal Saleh Mohammed; resources, Kareem Ali Jasim; data curation, Muayed Khaleel Ibrahim; writing—original draft preparation, Muayed Khaleel Ibrahim; writing—review and editing, Mudatheer M. Al-Slivani; supervision, Mudatheer M. Al-Slivani. All authors reviewed and approved the final version of the manuscript.

Availability of Data and Materials: The data that support the findings of this study are available from the Corresponding Author, Mudatheer M. Al-Slivani, upon reasonable request.

Ethics Approval: Not applicable.

Conflicts of Interest: The authors declare no conflicts of interest.

Abbreviations

The following abbreviations are used in this manuscript

Term	Interpretation
DC	Direct Current
SEM	Scanning Electron Microscopy
DOS	Density of States
ΔE	Band tail width/Width of the energy tail
ΔE_1, ΔE_2, ΔE_3	Activation energies for DC conduction
σ_{01}, σ_{02}, σ_{03}	Pre-exponential factors
T	Absolute temperature
k_β	Boltzmann's constant
$N(E_{ext})$	Density of extended states
$N(E_{loc})$/N(los)	Density of localized states
$N(E_F)$	Density of states near the Fermi level
R	Hopping distance
a	Atomic distance
e	Electron charge
νph	Phonon frequency

References

1. Wang H, Pei Y, LaLonde AD, Snyder GJ. Heavily doped p-type PbSe with high thermoelectric performance: an alternative for PbTe. Adv Mater. 2011;23(11):1366–70. [CrossRef].
2. Wu D, Zhao LD, Tong S, Li W, Wu L, Tan Q, et al. Superior thermoelectric performance in PbTe-PbS pseudo-binary system: extremely low thermal conductivity and enhanced power factor. J Am Chem Soc. 2014;136(32):11412–9. [CrossRef].
3. Pei Y, LaLonde AD, Wang H, Snyder GJ. Low effective mass leading to high thermoelectric performance. Energy Environ Sci. 2012;5(7):7963–9. [CrossRef].
4. Chen CL, Wang H, Chen YY, Day T, Snyder GJ. Thermoelectric properties of p-type polycrystalline SnSe doped with Ag. J Mater Chem A. 2014;2(29):11171–6. [CrossRef].
5. Ronneberger I, Zanolli Z, Wuttig M, Mazzarello R. Changes in the bonding nature during crystallization of Ge-Sb-Te alloys. Adv Mater. 2020;32(40):2001033. [CrossRef].
6. Gui X, Piva MM, Baumbach RE, Xie W. High-mobility electronic transport in the transition-metal chalcogenide $MoTe_2$. Inorg Chem. 2020;59(9):5798–802. [CrossRef].
7. Zhang JJ, Guan J, Dong S, Yakobson BI. Room-temperature ferroelectricity in group-IV metal chalcogenide nanowires. J Am Chem Soc. 2019;141(38):15040–5. [CrossRef].
8. Ning CZ, Dou L, Yang P. Bandgap engineering in semiconductor alloy nanomaterials with widely tunable compositions. Nat Rev Mater. 2017;2:17070. [CrossRef].
9. Hu L, Wu HJ, Zhu T, Fu C, He JQ, Ying PJ, et al. High thermoelectric performance of n-type SnSe polycrystals through Bi-doping-induced modulation of carrier concentration and band structure. Adv Energy Mater. 2018;8(29):1802116. [CrossRef].
10. Abrikosov NK, Avilov ES, Shelimova LE. Physico-chemical study of alloys of the GeTe-MnTe-PbTe system in the region of solid solutions based on GeTe. Neorg Mater. 1979;15(10):1757–61.
11. Gelbstein Y, Dashevsky Z, Dariel MP. High performance n-type PbTe-based materials for thermoelectric applications. Phys B Condens Matter. 2005;363(1–4):196–205. [CrossRef].
12. Hong BK, Kim IH. Effects of double doping germanium and indium on the thermoelectric properties of permingeatite. Korean J Met Mater. 2023;61(7):489–99. [CrossRef].

13. Azzawi JH, Al-Zahraa YA, Abdulmajeed MA, Jasim KA, Muravitskaya A, Al-Hamadani AA, et al. Gamma radiation dose's impact on the energy states and structural properties of $Se_{70}Ge_{20}Sb_{10}$ alloy. Chalcogenide Lett. 2025;22(7):593–601. [CrossRef].
14. Mohammed JS, Jasim KA, Hussein HS, Hussein AS. Structural and optical properties of SnTe1-xSex thin films prepared by thermal evaporation technique. Chalcogenide Lett. 2023;20(7):449–58. [CrossRef].
15. Priyadarshini P, Das S, Naik R. A review on metal-doped chalcogenide films and their effect on various optoelectronic properties for different applications. RSC Adv. 2022;12(16):9599–620. [CrossRef].
16. Bose S. Semiconductor quantum nanostructures for optoelectronic applications [dissertation]. Nanyang, China: Nanyang Technological University; 2018. [CrossRef].
17. Davis EA, Mott NF. Conduction in non-crystalline systems V. Conductivity, optical absorption and photoconductivity in amorphous semiconductors. Philos Mag A J Theor Exp Appl Phys. 1970;22(179):903–22. [CrossRef].
18. Mohammed MA, Aklo KN, Watan AW, Jasim KA, Salman EM. Effect of thermal neutron radiation dose on density of local and extended energy states in $Se_{55}S_{20}Sb_{15}Sn_{10}$ alloy. Iraqi J Appl Phys. 2024;20(2B):393–8.
19. Deepika, Singh H, Rathore KS, Saxena NS. Study of the electrical and optical properties of $Ge_{27}Se_{58}Pb_{15}$ chalcogenide glass. J Asian Ceram Soc. 2018;6(1):30–6. [CrossRef].
20. Wadi KM, Hasan MA, Aneed SH, Faraj MG, Jasim KA. Synthesis and analysis of the density states and optical characteristics of Se100-X TeX semiconductors. Aro Sci J Koya Univ. 2025;13(1):175–84. [CrossRef].
21. Kurnosov A, Lubchenko V. The mechanism of electrical conduction in glassy semiconductors. Proc Natl Acad Sci U S A. 2025;122(10):e2414650122. [CrossRef].
22. Kastner M. Pressure dependence of the absorption edge of amorphous selenium and As_2Se_3. Phys Rev Lett. 1972;28(6):355–7. [CrossRef].
23. Tang G. Polycrystalline SnSe thermoelectrics: new opportunity and challenge. MatLab. 2024;4(1):240013. [CrossRef].
24. Chaudhuri D, O'Donovan M, Streckenbach T, Marquardt O, Farrell P, Patra SK, et al. Multiscale simulations of the electronic structure of III-nitride quantum wells with varied indium content: connecting atomistic and continuum-based models. J Appl Phys. 2021;129(7):073104. [CrossRef].
25. Halenkovič T, Němec P, Nazabal V. Cluster-based DFT modeling of Raman vibrations in tetrahedral GeS_2 and $GeSe_2$ amorphous chalcogenides. Sci Rep. 2026;16:10009. [CrossRef].
26. Wang L, Zhang W, Back SY, Kawamoto N, Nguyen DH, Mori T. High-performance Mg_3Sb_2-based thermoelectrics with reduced structural disorder and microstructure evolution. Nat Commun. 2024;15(1):51120–1. [CrossRef].
27. Bischoff C, Schuller K, Martin SW. Short range structural models of the glass transition temperatures and densities of $0.5Na_2S + 0.5[xGeS_2 + (1 - x)PS_{5/2}]$ mixed glass former glasses. J Phys Chem B. 2014;118(13):3710–9. [CrossRef].
28. Houssa M, Scalise E, Sankaran K, Pourtois G, Afanas'ev VV, Stesmans A. Electronic properties of hydrogenated silicene and germanene. Appl Phys Lett. 2011;98(22):223107. [CrossRef].
29. Han WH, Chang KJ. Band-structure engineering of SnSe for high thermoelectric performance. Phys Rev Appl. 2016;6(4):044011. [CrossRef].
30. Jang H, Abbey S, Frimpong B, Nguyen CV, Ziolkowski P, Oppitz G, et al. Comparative study of thermoelectric properties of $Sb_2Si_2Te_6$ and $Bi_2Si_2Te_6$. ACS Appl Mater Interfaces. 2022;14(1):1270–9. [CrossRef].
31. Zhao H, Zhu J, Zhu Z, Bo L, Wang W, Liu X, et al. Effects of Ge-doping on thermoelectric performance of amorphous cubic $Sn_{0.5}Ag_{0.25}Bi_{0.25}Se_{0.50}Te_{0.50}$. Crystals. 2025;15(7):622. [CrossRef].